

Tuning the Activity of Zn(II) Complexes in DNA Cleavage: Clues for Design of New Efficient Metallo-Hydrolases

Carla Bazzicalupi,^{*,†} Andrea Bencini,^{*,†} Claudia Bonaccini,[‡] Claudia Giorgi,[†] Paola Gratteri,^{*,‡} Stefano Moro,[§] Manlio Palumbo,[§] Alessandro Simionato,[§] Jacopo Sgrignani,[‡] Claudia Sissi,^{*,§} and Barbara Valtancoli[†]

Dipartimento di Chimica, Università degli Studi di Firenze, Via della Lastruccia 3, 50019, Sesto Fiorentino, Firenze, Italy, Laboratorio di Molecular Modeling, Cheminformatics and QSAR, Dipartimento di Scienze Farmaceutiche, Laboratorio di Progettazione, Sintesi e Studio di Eterocicli Biologicamente Attivi, Polo Scientifico, Università degli Studi di Firenze, Via Ugo Schiff, 6, 50019 Sesto Fiorentino (FI), Italy, and Dipartimento di Scienze Farmaceutiche, Università degli Studi di Padova, Via Marzolo 5, 35131 Padova, Italy

Received January 17, 2008

The hydrolytic ability toward plasmid DNA of a mononuclear and a binuclear Zn(II) complex with two macrocyclic ligands, containing respectively a phenanthroline (L1) and a dipyridine moiety (L2), was analyzed at different pH values and compared with their activity in bis(*p*-nitrophenyl)phosphate (BNPP) cleavage. Only the most nucleophilic species $[ZnL1(OH)]^+$ and $[Zn_2L2(OH)_2]^{2+}$, present in solution at alkaline pH values, are active in BNPP cleavage, and the dinuclear L2 complex is remarkably more active than the mononuclear L1 one. Circular dichroism and unwinding experiments show that both complexes interact with DNA in a nonintercalative mode. Experiments with supercoiled plasmid DNA show that both complexes can cleave DNA at neutral pH, where the L1 and L2 complexes display a similar reactivity. Conversely, the pH-dependence of their cleavage ability is remarkably different. The reactivity of the mononuclear complex, in fact, decreases with pH while that of the dinuclear one is enhanced at alkaline pH values. The efficiency of the two complexes in DNA cleavage at different pH values was elucidated by means of a quantum mechanics/molecular mechanics (QM/MM) study on the adducts between DNA and the different complexed species present in solution.

Introduction

The development of genome analytical methods has recently increased the importance of DNA and RNA cleavage because of its biotechnological and medical applications in the manipulation of genes, the design of structural probes, and the development of novel therapeutic agents. Cleavage can be obtained through both chemical¹ and enzymatic methods,² the latter being those more often applied. Actually, nucleases or restriction enzymes are able to ensure rapid breaks and, in some instances, structure and/or sequence specificity. However, enzymatic methods are featured by a limited natural repertoire of target sequences, which severely hamper their applications.³

On the other hand, chemical methods allow the use of a wide range of experimental conditions such as pH, temperature, and salt concentration, which may on the contrary limit

- (1) (a) Boerner, L. J. K.; Zaleski, J. M. *Curr. Opin. Chem. Biol.* **2005**, *9*, 135–144. (b) Schneider, H.-J.; Yatsimirsky, A. In *Metal Ion in Biological Systems*; Sigel, H., Sigel, A., Eds.; Marcel Dekker: New York, 2003; Vol. 40, pp 369–462. (c) Komiyama, M. In *Metal Ions in Biological Systems*; Sigel, H., Sigel, A., Eds.; Marcel Dekker: New York, 2003; Vol. 40, pp 463–475. (d) Blasko, A.; Bruce, T. C. *Acc. Chem. Res.* **1999**, *32*, 475–484; and references therein. (e) Hegg, E. L.; Burstyn, J. N. *Coord. Chem. Rev.* **1998**, *173*, 133–165; and references therein. (f) Krämer, R. *Coord. Chem. Rev.* **1999**, *182*, 243–261, and references therein. (g) Kimura, E. *Curr. Op. Chem. Biol.* **2000**, *4*, 207–213. (h) Aoki, S.; Kimura, E. *Rev. Mol. Biotechnol.* **2002**, *90*, 129–155; and references therein. (i) Molenveld, P.; Engbersen, J. F. J.; Reinhoudt, D. N. *Chem. Soc. Rev.* **2000**, *29*, 75–86. (j) Williams, N. H.; Takasaki, B.; Wall, M.; Chin, J. *Acc. Chem. Res.* **1999**, *32* (6), 485–493. (k) Liu, C.; Wang, M.; Zhang, T.; Sun, H. *Coord. Chem. Rev.* **2004**, *248*, 147–168; and references therein. (l) Parkin, G. *Chem. Rev.* **2004**, *104*, 699–768. (m) Weston, J. *Chem. Rev.* **2005**, *105* (6), 2151–2174. (n) Chin, J. *Curr. Op. Chem. Biol.* **1997**, *1*, 514–521. (o) Scrimin, P.; Baltzer, L. *Curr. Op. Chem. Biol.* **2005**, *9* (6), 620–621. (p) Mancin, F.; Scrimin, P.; Tecilla, P.; Tonellato, U. *Chem. Commun.* **2005**, *20*, 2540–2548. (q) Mancin, F.; Tecilla, P. *New J. Chem.* **2007**, *31*, 800–817.

* To whom correspondence should be addressed. E-mail: carla.bazzicalupi@unifi.it (C.B.), andrea.bencini@unifi.it (A.B.), paola.gratteri@unifi.it (P.G.), claudia.sissi@unipd.it (C.S.).

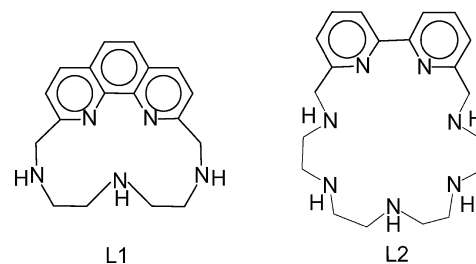
[†] Dipartimento di Chimica, Università degli Studi di Firenze.

[‡] Dipartimento di Scienze Farmaceutiche, Università degli Studi di Firenze.

[§] Dipartimento di Scienze Farmaceutiche, Università degli Studi di Padova.

the use of enzymatic techniques.⁴ Metal ions and complexes, because of their cationic character and three-dimensional structural profiles, have a natural aptitude to interact with DNA and may give rise to cleaving reactions. Several transition metal ions can be employed to derive efficient artificial metallonucleases which act through an oxidative pathway, for example, Cu(II),^{5–20} or through a hydrolytic mechanism, as in the case of Co(III),²¹ Fe(III),²² and lanthanide ions.^{1b,c,23–26} On the other hand, metal complexes containing Zn(II) are of particular interest, zinc being the most common metal ion in the active site of hydrolytic metalloenzymes. Many features of this metal, such as its

Scheme 1



L1

L2

ability in assisting Lewis activation, nucleophile generation, and leaving group stabilization, make Zn(II) ideal for the catalysis of hydrolytic reactions, including DNA cleavage. Actually, Zn(II)-bound hydroxo groups or activated free water molecules have been mentioned as potential nucleophilic agents in hydrolytic processes.^{27–32} Moreover, it has been shown that di- and trinuclear complexes generally display higher hydrolytic activity, thanks to the cooperative role played by the metals in the cleavage process.^{33–48}

We have recently reported a series of mono- and dinuclear Zn(II) complexes with polyamine ligands containing 1,10-phenanthroline or 2,2'-dipyridine, able to hydrolyze the phosphate ester bond of activated substrates, such as bis(*p*-nitrophenyl)phosphate (BNPP);⁴⁹ this study pointed out that the hydrolytic mechanism occurs through interaction of the anionic phosphate moiety with the Zn(II) centers and simultaneous attack of a nucleophilic Zn–OH function to phosphorus. The binuclear Zn(II) complex with ligand L2 (Scheme 1) proved to be one of the most efficient in BNPP hydrolysis, thanks to a bridging coordination of phosphate between the two metals, which gives rise to an increased activation of phosphorus to the nucleophilic attack.

It was also found that the heteroaromatic moiety reinforces the overall interaction between BNPP and the metal complex,

- (2) (a) Wu, J.; Kandavelou, K.; Chandrasegaran, S. *Cell. Mol. Life Sci.* **2007**, *64*, 2933–2944. (b) Hobartner, C.; Silverman, S. K. *Biopolymers* **2007**, *87*, 279–292. (c) Tachikawa, K.; Briggs, S. P. *Curr. Opin. Biotechnol.* **2006**, *17*, 659–665. (d) Chen, Z.; Zhao, H. *Nucleic Acids Res.* **2005**, *33*, e154. (e) McClelland, S. E.; Dryden, D. T. F.; Szczelkun, M. D. *J. Mol. Biol.* **2005**, *348*, 895–915. (f) van den Broek, B.; Noom, M. C.; Wuite, G. J. L. *Nucleic Acids Res.* **2005**, *33*, 2676–2684. (g) Katsura, S.; Harada, N.; Maeda, Y.; Komatsu, J.; Matsura, S.; Takashima, K.; Mizuno, A. *J. Biosci. Bioeng.* **2004**, *98*, 293–297. (h) Oestergaard, V. H.; Giangiacomo, L.; Bjergbaek, L.; Knudsen, B. R. *J. Biol. Chem.* **2004**, *279*, 28093–28099.
- (3) Shigemori, Y.; Oishi, M. *Nucleic Acids Res.* **2004**, *32*, e4/1–e4/8; and references therein.
- (4) Lilley, D. M. *Methods Enzymol.* **1992**, *212*, 133–139.
- (5) Ren, R.; Yang, P.; Zheng, W.; Hua, Z. *Inorg. Chem.* **2000**, *39*, 5454–5463.
- (6) (a) Rammo, J.; Schneider, H. J. *Inorg. Chim. Acta* **1996**, *251*, 125–134. (b) Lomadze, N.; Schneider, H.-J.; Albelda, M. T.; Garcia-España, E.; Verdejo, B. *Org. Biomol. Chem.* **2006**, *4*, 1755–1759. Chand, D. K.; Schneider, H.-J.; Aguilar, J. A.; Escarti, F.; Garcia-España, E.; Luis, S. V. *Inorg. Chim. Acta* **2001**, *316*, 71–78.
- (7) (a) Maheswari, P. U.; Roy, S.; Den Dulck, H.; Barends, S.; Van Wezel, G.; Kozlevcar, B.; Gamez, P.; Reedijk, J. *J. Am. Chem. Soc.* **2006**, *128*, 710–711. (b) Maheswari, P. U.; Lappalainen, K.; Sfrégola, M.; Barends, S.; Gamez, P.; Turpeinen, U.; Mutikainen, I.; van Wezel, G. P.; Reedijk, J. *Dalton Trans.* **2007**, 3676–3683.
- (8) Zhu, L.; Dos Santos, O.; Koo, C. W.; Rybstein, M.; Pape, L.; Canary, J. W. *Inorg. Chem.* **2003**, *42*, 7912–7920.
- (9) (a) Bencini, A.; Berni, E.; Bianchi, A.; Giorgi, C.; Valtancoli, B.; Chand, D. K.; Schneider, H. J. *Dalton Trans.* **2003**, *5*, 793–800. (b) Chand, D. K.; Schneider, H. J.; Bencini, A.; Bianchi, A.; Giorgi, C.; Ciattini, S.; Valtancoli, B. *Chem.–Eur. J.* **2000**, *6*, 4001–4008.
- (10) Sissi, C.; Mancin, F.; Gatos, M.; Palumbo, M.; Tecilla, P.; Tonellato, U. *Inorg. Chem.* **2005**, *44*, 2310–2317.
- (11) Itoh, T.; Hisada, H.; Sumiya, T.; Hosono, M.; Usui, Y.; Fujii, Y. *Chem. Commun.* **1997**, 677–678.
- (12) Qian, J.; Gu, W.; Liu, H.; Gao, F.; Feng, L.; Yan, S.; Liao, D.; Cheng, P. *Dalton Trans.* **2007**, 1060–1066.
- (13) Rajendiran, V.; Karthik, R.; Palaniandavar, M.; Stoekli-Evans, H.; Periasamy, V. S.; Akbarsha, M. A.; Srinag, B. S.; Krishnamurthy, H. *Inorg. Chem.* **2007**, *46*, 8208–8221.
- (14) Lu, Z.-L.; Liu, C. T.; Neverov, A. A.; Brown, R. S. *J. Am. Chem. Soc.* **2007**, *129*, 11642–11652.
- (15) Uma, V.; Elango, M.; Nair, B. U. *Eur. J. Inorg. Chem.* **2007**, 3484–3490.
- (16) García-Giménez, J. L.; Alzuet, G.; González-Álvarez, M.; Castiñeiras, A.; Liu-González, M.; Borrás, J. *Inorg. Chem.* **2007**, *46*, 7178–7188.
- (17) (a) Jin, Y.; Lewis, M. A.; Gokhale, N. H.; Long, E. C.; Cowan, J. A. *J. Am. Chem. Soc.* **2007**, *129*, 8353–8361. (b) Jin, Y.; Cowan, J. A. *J. Am. Chem. Soc.* **2005**, *127*, 8408–8415.
- (18) Zhao, Y.; Zhu, J.; He, W.; Yang, Z.; Zhu, Y.; Li, Y.; Zhang, J.; Guo, Z. *Chem.–Eur. J.* **2006**, *12*, 6621–6629.
- (19) An, Y.; Tong, M.-L.; Ji, L.-N.; Mao, Z.-W. *Dalton Trans.* **2006**, 206, 6–2071.
- (20) (a) Pitié, M.; Burrows, C. J.; Meunier, B. *Nucleic Acids Res.* **2000**, *28*, 4856–4864. (b) Bales, B. C.; Kodama, T.; Weledji, Y. N.; Pitié, M.; Meunier, B.; Greenberg, M. M. *Nucleic Acids Res.* **2005**, *33*, 5371–5379.
- (21) Hettich, R.; Schneider, H. J. *J. Am. Chem. Soc.* **1997**, *119*, 5638–5647.
- (22) Liu, C.; Wang, M.; Zhang, T.; Sun, H. *Coord. Chem. Rev.* **2004**, *248*, 147–168.
- (23) Branum, M. E.; Tipton, A. K.; Adrienne, K.; Zhu, S.; Que, L., Jr. *J. Am. Chem. Soc.* **2001**, *123*, 898–1904.
- (24) (a) Sumaoka, J.; Takeda, N.; Okada, Y.; Takahashi, H.; Shigekawa, H.; Komiyama, M. *Nucleic Acids Symp. Ser.* **1998**, *39*, 137–138. (b) Sumaoka, J.; Furuki, K.; Kojima, Y.; Shibata, M.; Hirao, K.; Takeda, N.; Komiyama, M. *Nucleosides, Nucleotides Nucleic Acids* **2006**, *25* (4–6), 523–538. (c) Chen, W.; Komiyama, M. *ChemBioChem* **2005**, *6* (10), 1825–1830. (d) Yamamoto, Y.; Uehara, A.; Tomita, T.; Komiyama, M. *Nucleic Acids Res.* **2004**, *32* (19 > zprint>), e153/1–e153/7. (e) Komiyama, M.; Arishima, H.; Yokoyama, M.; Kitamura, Y.; Yamamoto, Y. *ChemBioChem* **2005**, *6* (1), 192–196. (f) Chen, W.; Kitamura, Y.; Zhou, J.; Sumaoka, J.; Komiyama, M. *J. Am. Chem. Soc.* **2004**, *126* (33), 10285–10291.
- (25) (a) Roigk, A.; Yescheulova, O. V.; Fedorov, Y. V.; Fedorova, O. A.; Gromov, S. P.; Schneider, H.-J. *Org. Lett.* **1999**, *1*, 833–835. (c) Roigk, A.; Hettich, R.; Schneider, H.-J. *Inorg. Chem.* **1998**, *37*, 751–756. (d) Ragunathan, K. G.; Schneider, H.-J. *Angew. Chem., Int. Ed. Engl.* **1996**, *35*, 1219–1221. (e) Rammo, J.; Hettich, R.; Roigk, A.; Schneider, H.-J. *Chem. Commun.* **1996**, *1*, 105–7.
- (26) (a) Hashimoto, S.; Nakamura, Y. *J. Chem. Commun.* **1995**, 1413–1414. (b) Hashimoto, S.; Nakamura, Y. *J. Chem. Soc., Perkin Trans. 1* **1996**, 2623–2628.
- (27) (a) Basile, L. A.; Raphael, A. L.; Barton, J. K. *J. Am. Chem. Soc.* **1987**, *109*, 7550–7551. (b) Aka, F. N.; Akkaya, M. S.; Akkaya, E. U. *J. Mol. Catal. A: Chem.* **2001**, *165*, 291–294. (c) Ichikawa, K.; Tarnai, M.; Uddin, M. K.; Nakata, K.; Sato, S. *J. Inorg. Biochem.* **2002**, *91*, 437–450.
- (28) (a) Fitzsimons, M. P.; Barton, J. K. *J. Am. Chem. Soc.* **1997**, *119*, 3379. (b) Copeland, K. D.; Fitzsimons, M. P.; Houser, R. P.; Barton, J. K. *Biochemistry* **2002**, *41*, 343–356.
- (29) (a) Sissi, C.; Rossi, P.; Felluga, F.; Formaggio, F.; Palumbo, M.; Tecilla, P.; Toniolo, C.; Scrimin, P. *J. Am. Chem. Soc.* **2001**, *123*, 3169–3170. (b) Bologgia, E.; Gatos, M.; Lucatello, L.; Mancin, F.; Moro, S.; Palumbo, M.; Sissi, C.; Tecilla, P.; Tonellato, U.; Zagotto, G. *J. Am. Chem. Soc.* **2004**, *126* (14), 4543–4549.

thanks to π -stacking and hydrophobic interaction with the *p*-nitrophenyl moieties of this substrate, leading to a marked increase of the hydrolysis rate. In this manuscript we compare the hydrolytic properties toward BNPP and DNA of the Zn(II) complexes with ligands L1 and L2, able to form respectively stable mono- and dinuclear Zn(II) complexes in aqueous solutions. In both L1 and L2 complexes, the metal ions display a coordination sphere not saturated by the ligand donors, and facile deprotonation of metal-bound water molecules affords nucleophilic hydroxo-complexes at slightly alkaline pH values, making them promising candidates as artificial nucleases. The observed different hydrolytic properties of the two complexes toward DNA have been elucidated in the light of molecular modeling studies on the species formed in solution using a hybrid quantum mechanics/molecular mechanics (QM/MM) approach.⁵⁰

- (30) Maheswari, P. U.; Barends, S.; Oezalp-Yaman, S.; de Hoog, P.; Casellas, H.; Teat, S. J.; Massera, C.; Lutz, M.; Spek, A. L.; van Wezel, G. P.; Gamez, P.; Reedijk, *Chem.–Eur. J.* **2007**, *13*, 5213–5222.
- (31) An, Y.; Lin, Y.-Y.; Wang, H.; Sun, H.-Z.; Tong, M.-L.; Ji, L.-N.; Mao, Z.-W. *Dalton Trans.* **2007**, 125, 0–1254.
- (32) Wilson, B.; Gude, L.; Fernandez, M.-J.; Lorente, A.; Grant, K. B. *Inorg. Chem.* **2005**, *44*, 6159–6173.
- (33) (a) Kimura, E.; Koike, T. *Inorg. Chem.* **1997**, *44*, 229–261. (b) Kimura, E.; Koike, T. *Chem. Commun.* **1998**, 149, 5–1500. (c) Fenton, D. E.; Okawa, H. *Chem. Ber.* **1997**, *130*, 433–442.
- (34) Molenveld, P.; Stikvoort, W. M. G.; Kooijman, H.; Spek, A. L.; Engbersen, J. F. J.; Reinhoudt, D. N. *J. Org. Chem.* **1999**, *64*, 3896.
- (35) (a) Rossi, P.; Felluga, F.; Tecilla, P.; Formaggio, F.; Crisma, M.; Toniolo, C.; Scrimin, P. *Biopolymers* **2000**, *55*, 496–501. (b) Sissi, C.; Rossi, P.; Felluga, F.; Formaggio, F.; Palumbo, M.; Tecilla, P.; Toniolo, C.; Scrimin, P. *J. Am. Chem. Soc.* **2001**, *123*, 3169–3170. (c) Sissi, C.; Mancin, F.; Palumbo, M.; Scrimin, P.; Tecilla, P.; Tonellato, U. *Nucleosides, Nucleotides Nucleic Acids* **2000**, *19* (8), 1265–1271.
- (36) (a) Iranzo, O.; Kovalevsky, A. Y.; Morrow, J. R.; Richard, J. P. *J. Am. Chem. Soc.* **2003**, *125*, 1988–1993. (b) Iranzo, O.; Elmer, T.; Richard, J. P.; Morrow, J. R. *Inorg. Chem.* **2003**, *42*, 7737–7746. (c) Yang, M.-Y.; Richard, J. P.; Morrow, J. R. *Chem. Commun.* **2003**, 2832–2833.
- (37) (a) Jurek, P.; Martell, A. E. *Inorg. Chim. Acta* **1999**, *287*, 47–51. (b) Luiz, M. T. B.; Szpoganicz, B.; Rizzoto, M.; Basallote, M. G.; Martell, A. E. *Inorg. Chim. Acta* **1999**, *287*, 134–141. (c) Kong, D.; Martell, A. E.; Reibenspies, J. *Inorg. Chim. Acta* **2002**, *333*, 7–14.
- (38) (a) Chapman, W. H., Jr.; Breslow, R. *J. Am. Chem. Soc.* **1995**, *117*, 5462–5469. (b) Leivers, M.; Breslow, R. *Bioorg. Chem.* **2001**, *29*, 345–356.
- (39) Kuzuya, A.; Mizoguchi, R.; Morisawa, F.; Machida, K.; Komiyama, M. *J. Am. Chem. Soc.* **2002**, *124* (24), 6887–6894.
- (40) Schneider, H.-J.; Hettich, R. *J. Am. Chem. Soc.* **1997**, *119*, 5638–5647.
- (41) (a) Bazzicalupi, C.; Bencini, A.; Bianchi, A.; Fusi, V.; Giorgi, C.; Paoletti, P.; Valtancoli, B.; Zanchi, D. *Inorg. Chem.* **1997**, *36*, 2784–2790. (b) Bazzicalupi, C.; Bencini, A.; Berni, E.; Bianchi, A.; Fedi, V.; Fusi, V.; Giorgi, G.; Paoletti, P.; Valtancoli, B. *Inorg. Chem.* **1999**, *38*, 4115–4122. (c) Bazzicalupi, C.; Bencini, A.; Berni, E.; Bianchi, A.; Giorgi, G.; Paoletti, P.; Valtancoli, B. *Inorg. Chem.* **1999**, *38*, 6323–6325.
- (42) Nihan, F.; Akkaya, M. S.; Akkaya, E. U. *J. Mol. Catal. A: Chem.* **2001**, *165*, 291–294.
- (43) (a) Li, S.-A.; Yang, D.-X.; Li, D.-F.; Huang, J.; Tang, W.-X. *New J. Chem.* **2002**, *26*, 1831–1837. (b) Li, S.-A.; Li, D. F.; Yang, D.-X.; Li, Y.-Z.; Huang, J.; Yu, K.-B.; Tang, W.-X. *Chem. Commun.* **2003**, 7, 880–881. (c) Yang, D.-X.; Li, S.-A.; Li, D.-F.; Xia, J.; Yu, K.-B.; Tang, W.-X. *J. Chem. Soc., Dalton Trans.* **2002**, 4042–4047.
- (44) Vichard, C.; Kaden, T. A. *Inorg. Chim. Acta* **2002**, *337*, 173–180.
- (45) (a) Kimura, E.; Kikuchi, M.; Kitamura, H.; Koike, T. *Chem.–Eur. J.* **1999**, *5*, 3113–3123. (b) Koike, T.; Takashige, M.; Kimura, E.; Fujioka, H.; Shiro, M. *Chem.–Eur. J.* **1996**, *2*, 617–623. (c) Aoki, S.; Sugimura, C.; Kimura, E. *J. Am. Chem. Soc.* **1998**, *120*, 10094–10102. (d) Koike, T.; Inoue, M.; Kimura, E.; Shiro, M. *J. Am. Chem. Soc.* **1996**, *118*, 3091–3099.

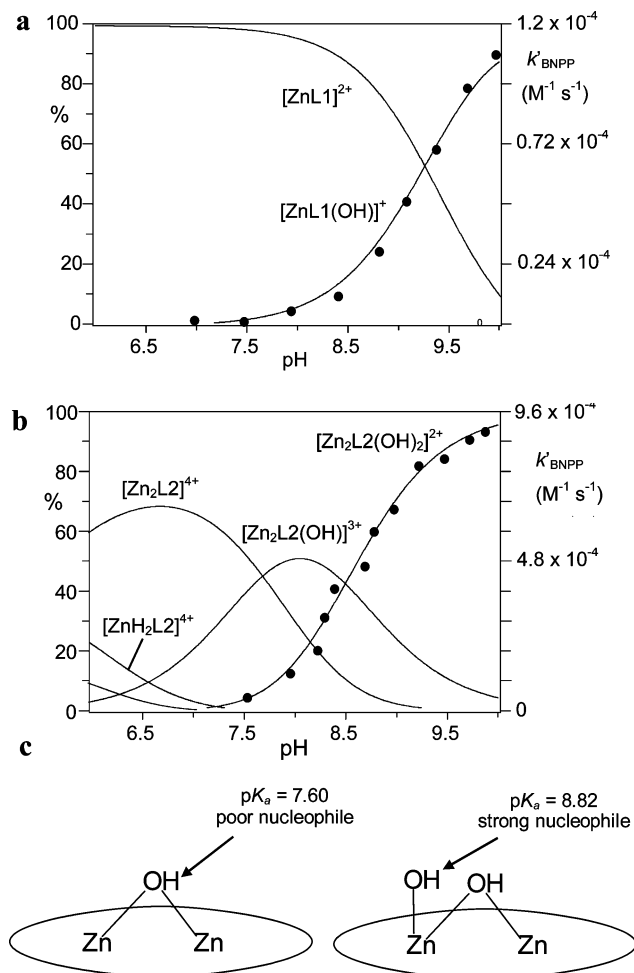


Figure 1. (a) Plot of the distribution curves of the L1 complexes (solid line, left y axis) and k_{BNPP} values for BNPP hydrolysis (•, right y axis) as a function of pH ($0.1 \text{ mol dm}^{-3} \text{ NMe}_4\text{NO}_3$, 308.1 K). (b) Plot of the distribution curves of the L2 dinuclear complexes (solid line, left y axis) and k_{BNPP} values for BNPP hydrolysis (•, right y axis) as a function of pH ($0.1 \text{ mol dm}^{-3} \text{ NMe}_4\text{NO}_3$, 308.1 K). (c) Sketch of the proposed structures for the $[\text{Zn}_2\text{L}_2(\text{OH})]^{3+}$ and $[\text{Zn}_2\text{L}_2(\text{OH})_2]^{2+}$ complexes.

Results

Bis(*p*-nitrophenyl) Phosphate Hydrolysis. L1 forms stable 1:1 complexes with Zn(II). As shown in Figure 1, Zn(II) complexation occurs at acidic pH values to give a $[\text{ZnL1}]^{2+}$ complex; then, deprotonation of a metal-bound water molecule in the alkaline pH region ($\text{pK}_a = 9.2$) affords

- (46) (a) Gajda, T.; Kramer, R.; Jancso, A. *Eur. J. Inorg. Chem.* **2000**, 1635–1644. (b) Jancso, A.; Mikkola, S.; Lönnberg, H.; Hegetschweiler, K.; Gaida, T. *Chem.–Eur. J.* **2003**, *9*, 5404–5415.
- (47) Qian, J.; Gu, W.; Liu, H.; Gao, F.; Feng, L.; Yan, S.; Liao, D.; Cheng, P. *Dalton Trans.* **2007**, 1060–1066.
- (48) Worm, K.; Chu, F. F.; Matsumoto, K.; Best, M. D.; Lynch, V.; Anslyn, E. V. *Chem.–Eur. J.* **2003**, *9*, 741–747.
- (49) (a) Bazzicalupi, C.; Bencini, A.; Berni, E.; Di Vaira, M. *Inorg. Chim. Acta* **2005**, *358*, 77–92. (b) Bazzicalupi, C.; Bencini, A.; Berni, E.; Bianchi, A.; Fornasari, P.; Giorgi, C.; Valtancoli, B. *Inorg. Chim. Acta* **2004**, *43*, 6255–6265. (c) Aguilar, J.; Bencini, A.; Berni, E.; Bianchi, A.; Garcia-España, E.; Gil, L.; Ruiz-Ramirez, L.; Soriano, C. *Eur. J. Inorg. Chem.* **2004**, 4061–4071.
- (50) (a) *Combined Quantum Mechanical and Molecular Mechanical Methods*; Gao, J., Thompson, M. A., Eds.; American Chemical Society: Washington, DC, 1998. (b) Monard, G.; Merz, K. M. *Acc. Chem. Res.* **1999**, *32*, 904–911. (c) Spiegel, K.; Magistrato, A. *Org. Biomol. Chem.* **2006**, *4*, 2507–2517; and references therein. (d) Friesner, R. A. *Adv. Protein Chem.* **2006**, *72*, 79–104. (e) Senn, H. M.; Thiel, W. *Curr. Opin. Chem. Biol.* **2007**, *11*, 182–187.

the monohydroxo-complex $[\text{ZnL1}(\text{OH})]^+$. The Zn(II) complex with L1 induces BNPP cleavage at alkaline pH values to give *p*-nitrophenate and mono(*p*-nitrophenyl) phosphate.⁵¹ The rate constants for BNPP hydrolysis to give MNPP and NP in the presence of the L1 complex was spectrophotometrically determined at different pH values by an initial slope method, monitoring the time evolution of the NP band at 403 nm. Figure 1a reports the pH dependence of the rate constant values (k_{BNPP}) in the pH range 6–10, superimposed to the corresponding distribution diagram. BNPP cleavage is promoted only by the $[\text{ZnL1}(\text{OH})]^+$ hydroxo-complex, while the $[\text{ZnL}]^{2+}$ is not active. A plot of the k_{BNPP} values as a function of the concentration of $[\text{ZnL1}(\text{OH})]^+$ allowed us to determine the k'_{BNPP} value for 100% formation of the active species (see Experimental Section), which was found to be $1.2 \times 10^{-4} \text{ M}^{-1} \text{ s}^{-1}$.

Considering Zn(II) complexation with L2, previous work^{49b} has shown that the ligand forms a $[\text{Zn}_2\text{L}_2]^{4+}$ dinuclear complex at slightly acidic pH values and the two hydroxo species $[\text{Zn}_2\text{L}_2(\text{OH})]^{3+}$ and $[\text{Zn}_2\text{L}_2(\text{OH})_2]^{2+}$, with $\text{p}K_a$ values of 7.60 and 8.82, respectively, in the alkaline pH region (Figure 1b).⁵² The particularly low value of $\text{p}K_a$ for the formation of the $[\text{Zn}_2\text{L}_2(\text{OH})]^{3+}$ complex was attributed to the assembly within the macrocyclic cavity of a $\text{Zn}_2(\mu\text{-OH})$ unit, a poor nucleophilic agent because of the simultaneous interaction of hydroxide with two electrophilic metal centers. Conversely, the higher $\text{p}K_a$ value for the formation of $[\text{Zn}_2\text{L}_2(\text{OH})_2]^{2+}$ suggested that in this complex one of the hydroxide anions is likely to be bound to a single Zn(II) ion (Figure 1c) to afford a more potent nucleophilic function.^{49b} Actually, only the dihydroxo complex $[\text{Zn}_2\text{L}_2(\text{OH})_2]^{2+}$ promotes BNPP hydrolysis in aqueous solution ($k'_{\text{BNPP}} = 9.6 \times 10^{-4} \text{ M}^{-1} \text{ s}^{-1}$), while the $[\text{Zn}_2\text{L}_2]^{4+}$ and the $[\text{Zn}_2\text{L}_2(\text{OH})]^{3+}$ species are totally inactive (Figure 1b).^{49b} Of note, the dinuclear L2 complex $[\text{Zn}_2\text{L}_2(\text{OH})_2]^{2+}$ exhibits a remarkable hydrolytic ability with a second-order rate constant for BNPP cleavage about 8 times higher than that of the mononuclear $[\text{ZnL1}]^{2+}$ complex.

DNA Binding Studies. The DNA binding properties of the test ligands were investigated by means of UV and circular dichroism (CD) spectroscopy and unwinding experiments. Unfortunately, L2 and its dinuclear complex absorb below 300 nm thus preventing us from performing accurate spectroscopic titrations. Similarly, L1 and its complex exhibit

an absorption band at about 320 nm with low intensity ($\epsilon = 960 \text{ M}^{-1} \text{ cm}^{-1}$) and poorly affected by the presence of the nucleic acid.

The CD spectra of ctDNA were therefore monitored at increasing ligand or complex concentrations. In the presence of L1 or its Zn^{2+} complex, the dichroic signal at 275 nm progressively increased up to $15000 \text{ deg} \times \text{cm}^2 \times \text{dmol}^{-1}$ (mean residue ellipticity) at a complex concentration corresponding to 20–30 μM . Further additions of the test compound induced signal decrease. When L2 was used, a remarkable reduction in CD intensity was observed in the low micromolar range. Parallel measurements showed light scattering produced by DNA solutions containing the complex in $\approx 20 \mu\text{M}$ concentration. These results suggest that L2 can efficiently induce DNA condensation. The described phenomena are occurring both in the presence and in the absence of Zn^{2+} . As already reported for other polyamine compounds, we can relate this behavior to the basic character of this polyazamacrocyclic.

Because the tested ligands present an aromatic moiety, an intercalative DNA binding mode could be inferred. To assess this point supercoiled plasmid was incubated with increasing concentrations of the complexes in the presence of Topoisomerase I. The absence of the supercoiled form of the plasmid after ligand removal indicates that the complexes do not efficiently intercalate into the DNA double helix.

DNA Cleavage. The ability of the complexes with L1 and L2 to induce DNA cleavage was assessed on supercoiled plasmid DNA. When pBR 322 was incubated with ligands in the absence of metal ions in 20 mM HEPES at pH 7.0, no change in its electrophoretic mobility was observed, supporting the absence of any cleavage activity. On the contrary, the formation of nicked circular DNA (form II) was observed upon addition of 1 equiv and 2 equiv of Zn^{2+} to buffered solutions of L1 and L2 at pH 7, respectively. In our experimental conditions, no linear DNA (form III) was observed. As shown in Figure 2, the extent of DNA cleavage depends on the nature and concentration of the complex, with a clear increase of generated form II with increasing concentration of the mononuclear and dinuclear complexes with L1 and L2, respectively. At this pH value, the two complexes display a similar hydrolytic efficiency. DNA is completely cleaved in the presence of the dinuclear complex with L2 at 10 μM concentration, while higher complex concentrations lead to DNA precipitation. Formation of nicked DNA by the L1 complex is almost linearly related to its concentration up to a 1:10 molar ratio (in this condition DNA is cleaved in ca. 80%) and then shows a minor increase at higher complex concentrations.

To gain further insight into the mechanism(s) of DNA cleavage, we analyzed the activity of the two metal complexes at different pH values, and the results are summarized in Figure 3. Actually, the reactivity of both complexes depends on pH.

In the case of the mononuclear complex with L1, a decrease of activity in DNA cleavage with increasing pH is observed for low complex concentrations ($< 2 \mu\text{M}$). In these conditions, the highest complex activity is observed at pH

(51) The products of BNPP hydrolysis were identified by means of ^1H and ^{31}P NMR measurements. The ^1H NMR spectrum recorded after mixing BNPP and the Zn(II) complex at pH 9 shows the appearance of the signals of *p*-nitrophenate, NP (two doublets at 6.72 and 8.28 ppm), and of mono(*p*-nitrophenyl) phosphate, MNPP (two doublets at 7.29 and 8.20 ppm). Integration of the signals accounts for a 1:1 molar ratio between the NP and MNPP formed in the hydrolytic process. At the same time, the signal of MNPP (a singlet at 0.6 ppm) appears in the ^{31}P spectrum. The time evolution of the ^{31}P spectra shows a progressive increase of intensity of this signal and a simultaneous decrease of the BNPP signal. No other signal, including that of inorganic phosphate at 3.79 ppm, was observed in ^{31}P NMR spectra, even for prolonged reaction times, indicating that the MNPP is not further hydrolyzed by the Zn(II) complexes.

(52) The $\text{p}K_a$ values of 7.60 and 8.82 refer to the equilibria $[\text{Zn}_2\text{L}_2]^{4+} + \text{H}_2\text{O} = [\text{Zn}_2\text{L}_2(\text{OH})]^{3+} + \text{H}^+$ and $[\text{Zn}_2\text{L}_2(\text{OH})]^{3+} + \text{H}_2\text{O} = [\text{Zn}_2\text{L}_2(\text{OH})_2]^{2+} + \text{H}^+$, respectively.

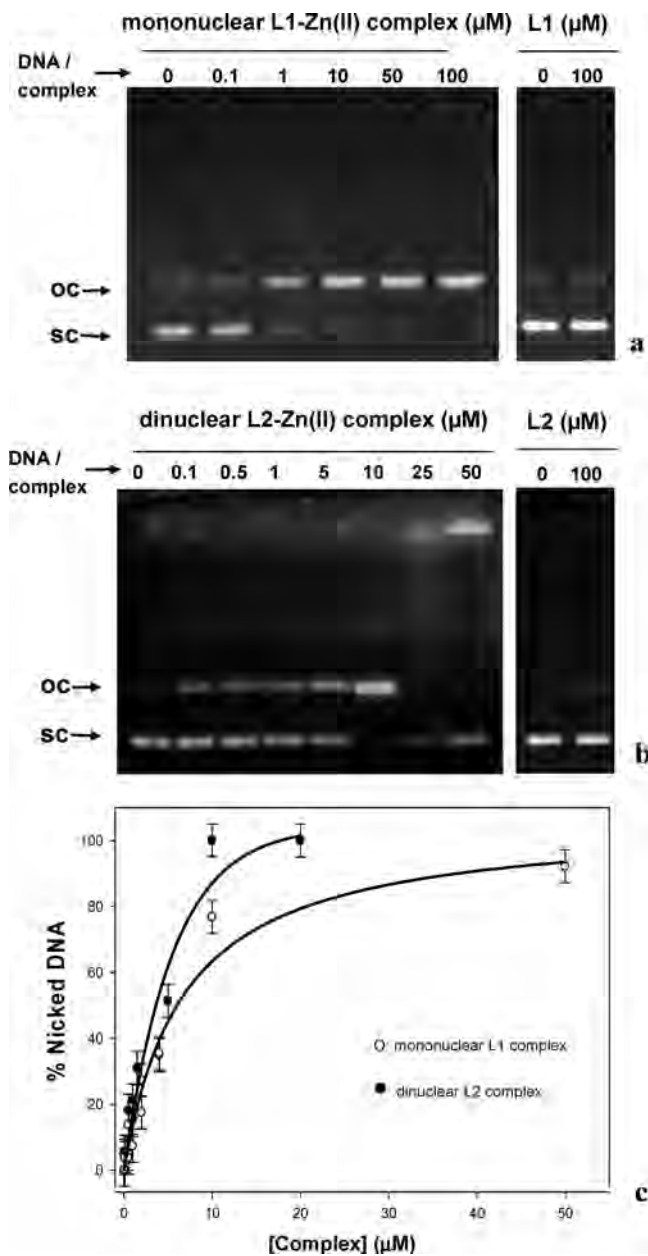


Figure 2. Cleavage of pBR 322 (agarose electrophoresis of the cleavage reaction products) induced by increasing concentrations of the L1 (a) and L2 (b) complexes in 20 mM Hepes at pH 7.0 (24 h incubation at 37 °C; sc: supercoiled plasmid, oc: open circular form (Nicked DNA); the last two lines on the right are relative to control measurements on pBR 322 alone (0) and in the presence of the ligands (100 μM) in the absence of Zn²⁺) and plot of the percentage of the nicked form of DNA as a function of the concentrations of the L1 and L2 complexes at pH 7.0 (c).

6, while at pH 9 DNA remains almost not cleaved. At higher complex concentration, the reactivity decreases in the order $7 > 8 > 6 \cong 9$. Actually, complete substrate conversion from supercoiled to nicked plasmid is observed only at pH 7 in the presence of a large amount of the complex (100 μM), while a much lower percentage of nicked DNA is formed at pH 6 and 9. If at pH 9.0 this behavior can be ascribed to poor reactivity, the same is not true at pH 6.0, where the high reactivity observed at low complex concentrations is followed by a leveling off of the percentage of cleaved DNA. This accounts for a template effect or for a change in DNA conformation in the presence of high

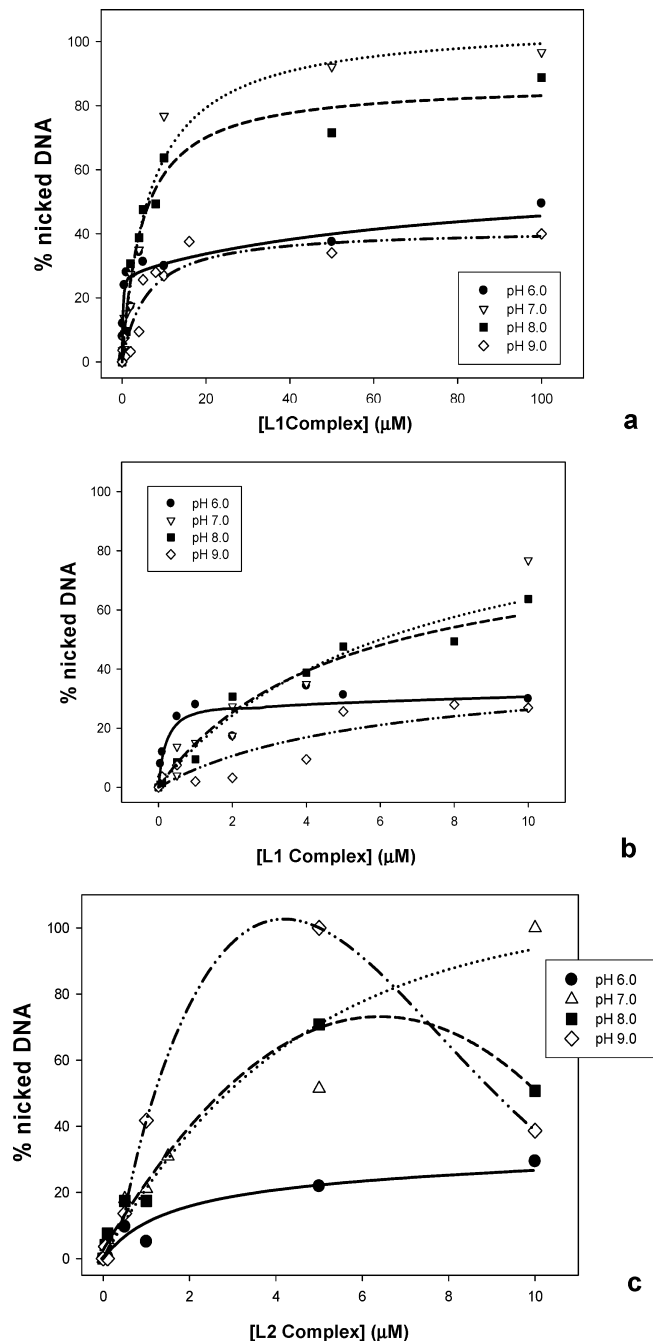


Figure 3. Plot of the percentages of nicked DNA in the presence of increasing amounts of the L1 complex at different pH values (a), enlarged view of the plot for low molar concentrations of the L1 complex (b), and plot of the percentages of nicked DNA in the presence of increasing amounts of the L2 complex at different pH values (c).

amounts of the complex at pH 6, which prevents the reactive moiety from being properly located with respect to the phosphate group.

The dinuclear complex with L2 displays a different behavior in DNA cleavage. In fact, as shown in Figure 3, for low complex concentrations (<5 μM) the reactivity increases in the order $6 < 7 \cong 8 < 9$, that is, the opposite trend observed for the L1 complex. By incrementing complex concentration, a marked decrease of reactivity is observed at pH 8 and 9. This can be related to the condensation effects cited above, which could prevent DNA cleavage. Indeed, at

all pH tested, complex concentrations higher than 20 μM induce DNA precipitation.

Molecular Modeling Studies. To elucidate the binding mode of the L1 and L2 complexes with DNA, we carried out a molecular modeling study on their interaction with the DNA decanucleotide duplex d(5'-GCGCGCGCGC-3'), by using a hybrid quantum mechanics/molecular mechanics (QM/MM) study. For both complexes the modeling study was focused mainly on a nonintercalative DNA binding mode because the possible intercalation was ruled out in the light of unwinding experiments (see above).

Mononuclear L1 Complex/d-(GCGCGCGCGC) Adduct. Modeling studies were carried out on the $[\text{ZnL1}]^{2+}$ and $[\text{ZnL1}(\text{OH})]^+$ complexes, formed in solution in the pH range 6–9 (Figure 1).

In the case of the $[\text{ZnL1}]^{2+}$ complex, we used as starting coordinates for the docking procedure those of the $[\text{ZnL1}(\text{H}_2\text{O})]^{2+}$ cation, derived from the X-ray structure of the $[\text{ZnL1}(\text{H}_2\text{O})](\text{ClO}_4)_2$ salt (Figure 4a).⁵³ Other complexes, containing two coordinated water molecules, gave minimized structures at by far higher energy than $[\text{ZnL1}(\text{H}_2\text{O})]^{2+}$ and, therefore, they were neglected. In the $[\text{ZnL1}(\text{H}_2\text{O})]^{2+}$ complex, the metal is coordinated in a tetrahedral mode by the phenanthroline nitrogens, by the central secondary nitrogen of the aliphatic chain, and by an exogenous water molecule. The ligand assumes a bent conformation which leaves on the metal a large zone not occupied by the donor atoms and therefore available for anchoring an exogenous species, even in the presence of a Zn(II)-bound water molecule.^{49a} As a consequence, the coordinated water molecule was not removed during the docking and the QM/MM procedures.

The QM/MM optimized conformation for the $[\text{ZnL1}(\text{H}_2\text{O})]^{2+}$ /d-(5'-GCGCGCGCGC-3') adduct (Figure 4b,c) shows the metal complex inserted within the minor groove to give several Van der Waals interactions between the phenanthroline carbon atoms and, respectively, three and four nucleobases of the two DNA strands. The most interesting feature, however, is the presence of a phosphate oxygen at close distance, 2.14 Å, from the Zn(II) ion; the corresponding phosphorus is 4.07 Å apart from the coordinated oxygen of the water molecule.

In the case of the mononuclear hydroxo L1 complex, we considered species of the type $[\text{ZnL1}(\text{H}_2\text{O})(\text{OH})]^+$; a conformational search shows the presence of two main groups of conformers,^{49a} featured respectively by a *bent* conformation of the complex (Figure 5a), similar to that found in the crystal structure of the $[\text{ZnL1}(\text{H}_2\text{O})]^{2+}$ cation, or by a planar geometry of the macrocycle (Figure 5b). In both cases, in the minimized conformers the water molecule does not interact with the metal and was removed during the docking procedure to leave a free coordination site on the metal center.

The QM/MM treatment shows that both conformers are inserted in the minor groove, forming several Van der Waals

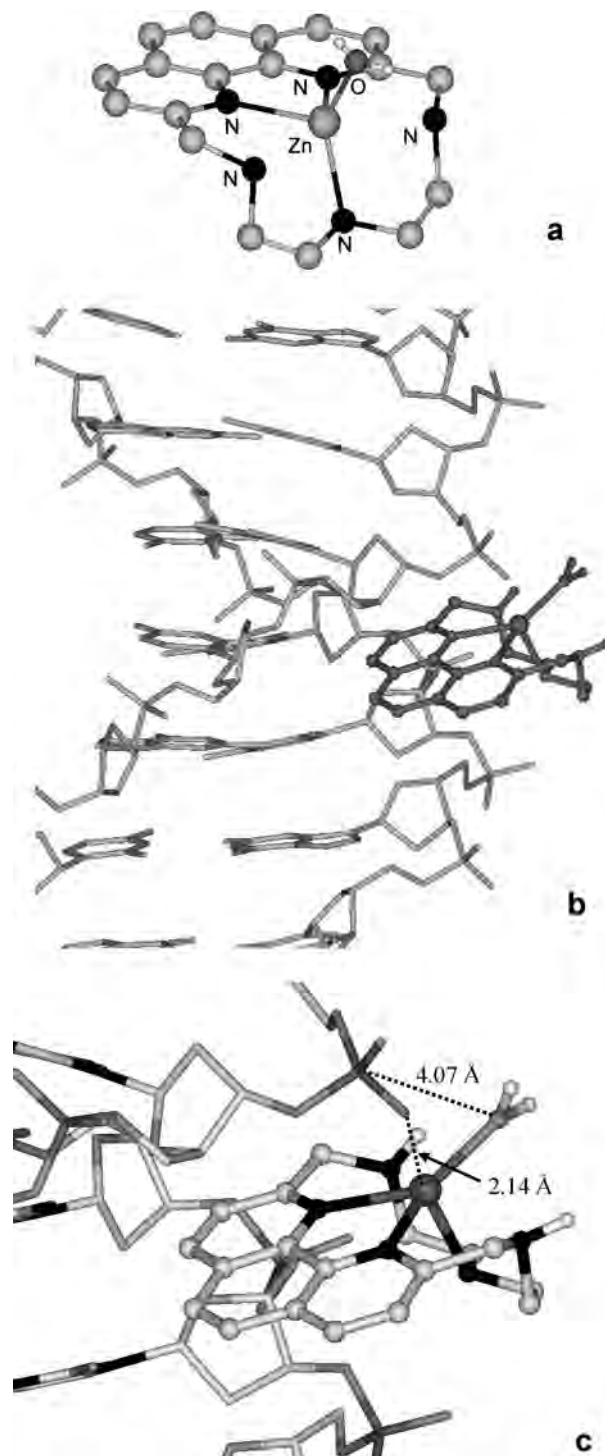


Figure 4. Crystal structure of the $[\text{ZnL1}(\text{H}_2\text{O})]^{2+}$ cation (a), low energy conformer for the $[\text{ZnL1}(\text{H}_2\text{O})]^{2+}$ /DNA adduct (b) with an enlarged view evidencing the interaction mode (c).

interactions involving mainly the phenanthroline moiety and three and four nucleobases belonging, respectively, to the two DNA strands (Figures 6 and 7). From an energetic point of view, however, the lowest energy QM/MM optimized DNA adduct of *planar*- $[\text{ZnL1}(\text{OH})]^+$ is remarkably more stable than the *bent*- $[\text{ZnL1}(\text{OH})]^+$ one ($\Delta E = 5.5$ kcal/mol), probably because of the unfavorable contribution of the electrostatic repulsion between the negatively charged hydroxo and phosphate groups, which are found at close

(53) Bazzicalupi, C.; Bencini, A.; Bianchi, A.; Giorgi, C.; Fusi, V.; Valtancoli, B.; Bernardo, M. A.; Pina, F. *Inorg. Chem.* **1999**, *38*, 3806–3816.

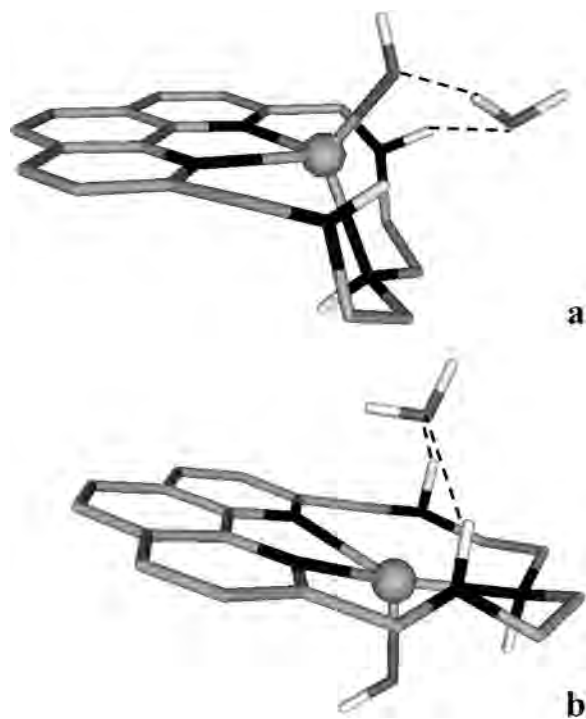


Figure 5. Lowest energy conformers of the *bent* (a) and *planar* (b) families for the $[\text{ZnL1}(\text{H}_2\text{O})(\text{OH})]^+$ complex. In the *bent* conformer the water lies 3.35 Å apart from the metal ion and gives hydrogen bonding with the hydroxide anion ($\text{OH}_2 \cdots \text{OH}$ 1.64 Å) and one amine group of the macrocycle ($\text{H}_2\text{O} \cdots \text{HN}$ 1.92 Å), while in the *planar* conformer the water lies 3.35 Å apart from the metal ion and gives hydrogen bonding with two amine groups of the macrocycle ($\text{H}_2\text{O} \cdots \text{HN}$ 2.47 and 2.42 Å).

distance in the *bent*- $[\text{ZnL1}(\text{OH})]^+$ adduct (Figure 6). In the *planar*- $[\text{ZnL1}(\text{OH})]^+$ /DNA adduct (Figure 7), a phosphate oxygen is located 2.56 Å far from the Zn(II) ion and lies on the opposite side of the macrocyclic complex with respect to the Zn-bound hydroxide. Hydrogen bonding interactions between the benzylic NH groups of the macrocyclic complex and the coordinated oxygen of the phosphate (N–HO distances 2.19 and 2.28 Å) reinforce the overall DNA/complex interaction.

The existence of a *planar* conformation for the $[\text{ZnL1}(\text{H}_2\text{O})]^{2+}$ /d-(5'-GCGCGCGCGC-3') adduct was also checked. However the QM/MM optimized structure was remarkable less stable (ΔE about 30 kcal/mol) than the *bent* conformation.

Binuclear L2 Complex/d-(GCGCGCGCGC) Adduct.

Modeling studies were carried out on the $[\text{Zn}_2\text{L2}]^{4+}$ complex and its hydroxo-derivatives $[\text{Zn}_2\text{L2}(\text{OH})]^{3+}$ and $[\text{Zn}_2\text{L2}(\text{OH})_2]^{2+}$, which are predominant in solution from slightly acidic to alkaline pH values (Figure 1). Considering $[\text{Zn}_2\text{L2}]^{4+}$, previous work showed that this complex contains a hydroxide anion bridging the two metals and a protonated nitrogen atom, affording an overall $[\text{Zn}_2\text{L2H}(\mu\text{-OH})]^{4+}$ stoichiometry;^{49b} therefore, in the docking procedure of $[\text{Zn}_2\text{L2}]^{4+}$, we used the coordinates of the $[\text{Zn}_2\text{L2H}(\mu\text{-OH})\text{Br}_2]^{2+}$ cation (Figure 8a), derived from the resolution of its crystal structure,^{49b} taking care to replace the mobile bromide anions with water molecules. The resulting $[\text{Zn}_2\text{L2H}(\mu\text{-OH})(\text{H}_2\text{O})_2]^{2+}$ cation was freely minimized. To obtain a free coordination position on the metal centers, the water molecules were then removed, one by one, from the

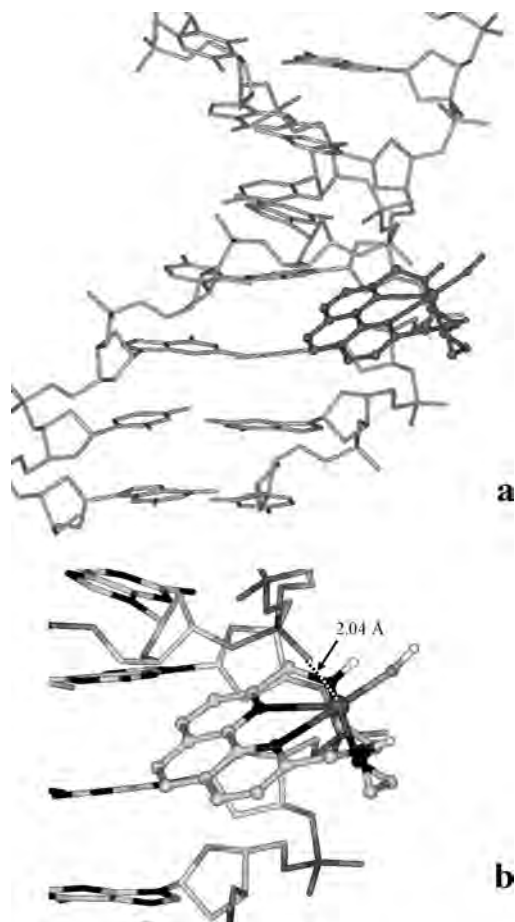


Figure 6. Lowest energy conformers of the *bent*- $[\text{ZnL1}(\text{OH})]^+$ /DNA adduct (a) with enlarged view showing the interaction mode (b).

$[\text{Zn}_2\text{L2H}(\mu\text{-OH})(\text{H}_2\text{O})_2]^{2+}$ complex during the docking and QM/MM procedures.

Interaction with DNA does not significantly change the complex conformation. In the lowest energy conformer (Figure 8b,c) a phosphate oxygen interacts very weakly with both metal ions, lying at 2.53 Å from the zinc atom bound to the heteroaromatic nitrogens and at 2.72 Å from the other one. Two hydrogen bonding contacts involving two NH groups of the macrocycle and two different oxygens of the phosphate strengthen the complex/DNA interaction (N \cdots HO distances 2.55 and 2.17 Å, Figure 8b,c). Differently from L1, the Zn(II) complex with L2 is not inserted within the minor groove and displays Van der Waals interactions with three nucleobases of a single strand. Furthermore, the bridging hydroxide group and the coordinated water molecule are located on the opposite side of the complex with respect to the phosphate group.

In the case of the $[\text{Zn}_2\text{L2}(\text{OH})]^{3+}$, the lowest energy conformer was obtained by removing the acidic proton from $[\text{Zn}_2\text{L2H}(\mu\text{-OH})(\text{H}_2\text{O})_2]^{2+}$ and then performing a conformational search, followed by QM optimization on the resulting $[\text{Zn}_2\text{L2}(\mu\text{-OH})(\text{H}_2\text{O})]^{3+}$ complex. As already done for $[\text{Zn}_2\text{L2H}(\mu\text{-OH})(\text{H}_2\text{O})_2]^{2+}$, the water molecules were removed, one by one, during the docking and the QM/MM procedures.

Differently from the $[\text{Zn}_2\text{L2H}(\mu\text{-OH})]^{2+}$ complex, in the resulting $[\text{Zn}_2\text{L2}(\mu\text{-OH})(\text{H}_2\text{O})]^{3+}$ /DNA adduct a single zinc ion of the complex strongly interacts with a phosphate

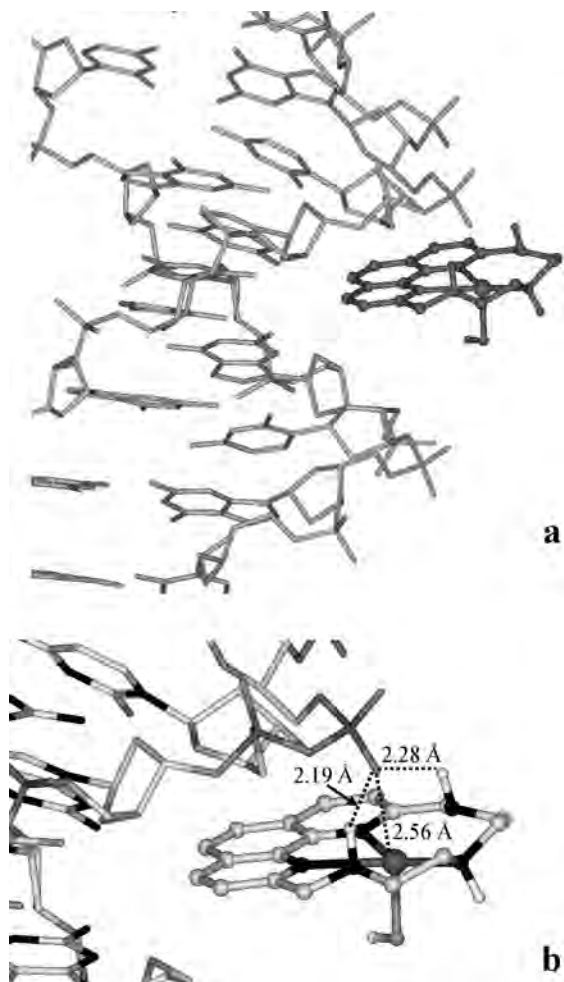


Figure 7. Lowest energy conformers of the *planar*-[ZnL1(OH)]⁺/DNA adduct (a) with enlarged view showing the interaction mode (b).

oxygen atom ($\text{Zn}\cdots\text{O}$ 2.16 Å), while a strong hydrogen bond between an amine group and a different phosphate oxygen ($\text{N}-\text{H}\cdots\text{O}-\text{P}$ 2.05 Å) reinforces the overall complex/DNA interaction (Figure 9). The complex is located outside the minor groove and gives Van der Waals contacts mainly involving the dipyrindine unit and the nucleobases of a single strand. Once again, the hydroxo group and the remaining water molecule are located in *trans* position with respect to the phosphate group.

Finally, the lowest energy conformer of the $[\text{Zn}_2\text{L2}(\text{OH})_2]^{2+}$ was obtained by removing a proton from one water molecule of $[\text{Zn}_2\text{L2}(\mu\text{-OH})(\text{H}_2\text{O})_2]^{3+}$ and performing a conformational search. Only a conformation of the resulting $[\text{Zn}_2\text{L2}(\mu\text{-OH})(\text{OH})(\text{H}_2\text{O})]^{2+}$ cation, containing a bridging hydroxide and a single-bound hydroxide, was successfully optimized by QM methods (see Supporting Information, Figure S1). The water molecule was then removed during the docking procedure. All the resulting poses for the $[\text{Zn}_2\text{L2}(\mu\text{-OH})(\text{OH})]^{2+}$ /DNA adduct are featured by a remarkable distance of the dizinc core from the phosphate. In the lowest energy pose, the aliphatic polyamine chain is partially inserted in the minor groove to give a hydrogen bonding contact between an amine group and phosphate (see Supporting Information, Figure S2). Both Zn(II) ions remain

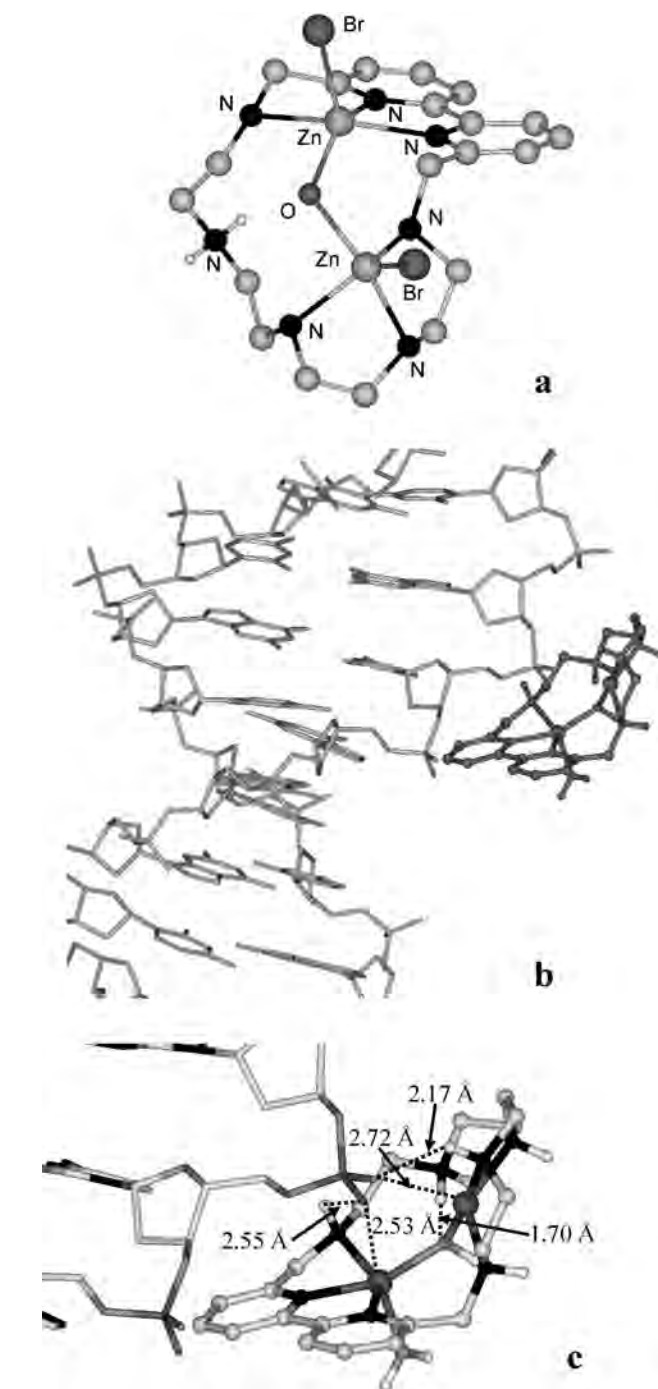


Figure 8. Crystal structure of the $[\text{Zn}_2\text{L2H}(\mu\text{-OH})\text{Br}_2]^+$ complex (a) and lowest energy conformer for $[\text{Zn}_2\text{L2H}(\mu\text{-OH})\text{H}_2\text{O}]^{4+}$ /DNA adduct (b) with enlarged view showing the interaction mode (c).

far from phosphate, the shortest P–OZn distance being about 5 Å

Discussion

It is accepted that the hydrolytic properties of a Zn(II) complex toward DNA or its model compounds depend mainly on activation of the phosphate group upon interaction with the metal, as well as on the nature of the nucleophilic species, most often metal-bound hydroxide anions and their concentrations in solutions. For instance, BNPP hydrolysis promoted by mono- and dinuclear Zn(II) complexes is

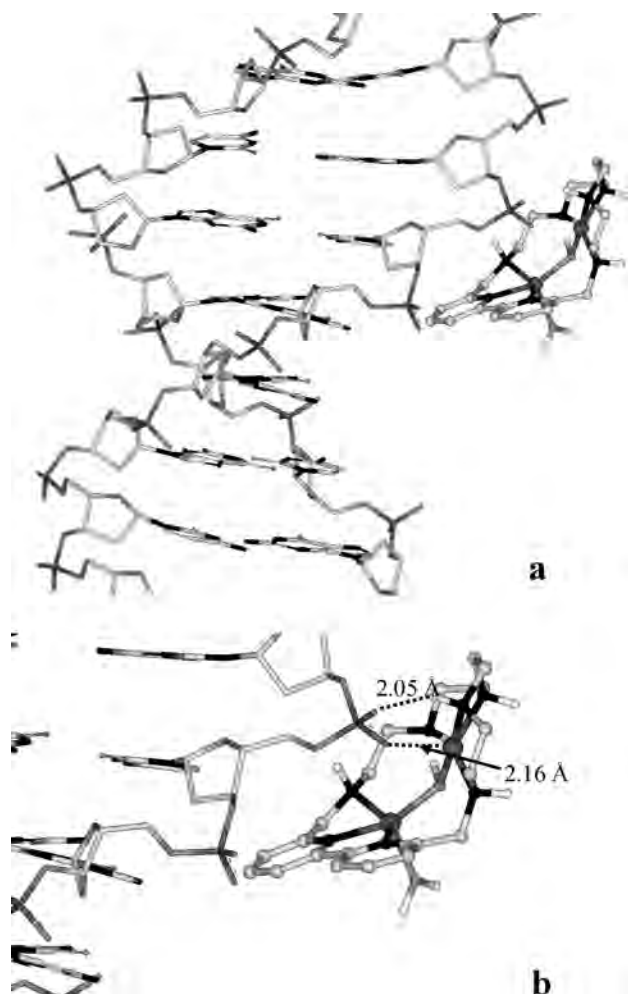


Figure 9. Lowest energy conformer for $[\text{Zn}_2\text{L}_2(\mu\text{-OH})(\text{H}_2\text{O})]^{3+}/\text{DNA}$ adduct (a) with enlarged view showing the interaction mode (b).

generally explained in terms of an “associative” mechanism,^{33–49} in which the substrate would approach the Zn(II) complex and the oxygens of BNPP start associating with the electrophilic Zn(II) ion while a zinc-bound hydroxide operates a nucleophilic attack at the phosphorus. The hydrolytic process is therefore favored by a strong interaction of the BNPP ester with the electrophilic metal centers and by a high nucleophilic character of the Zn–OH functions, that is, by high $\text{p}K_{\text{a}}$ values for the formation of the Zn-bound hydroxide.

However, other effects can influence the activity of the complex toward the phosphate ester bonds, such as hydrogen bonding between the complexes and the phosphate moieties, hydrophobic characteristics of the hydrolytic agent, and, in the case of DNA cleavage, intercalation between the nucleobases. In particular, these factors can determine the spatial disposition of the complex within the DNA backbone as well as the orientation of the nucleophilic functions in the DNA-complex adducts. Finally, metal-bound hydroxide anions or water molecules can act as general basic or general acid catalysts, respectively. In this respect, the L1 and L2 complexes display a coordination sphere of the metals not saturated by the ligands donors, with “free” binding sites available to interact with phosphate groups. Finally, both complexes possess heteroaromatic moieties and a number

of NH functions, which may reinforce the overall interaction with the substrates through hydrophobic and/or hydrogen bonding interactions.

For both L1 and L2 complexes, BNPP cleavage takes place in the alkaline pH region ($\text{pH} > 8$), where the hydrolytically active hydroxo-species $[\text{ZnL1}(\text{OH})]^+$ and $[\text{Zn}_2\text{L}_2(\text{OH})_2]^{2+}$ are formed in solution. The $[\text{ZnL1}]^{2+}$, $[\text{Zn}_2\text{L}_2]^{4+}$, and $[\text{Zn}_2\text{L}_2(\mu\text{-OH})]^{3+}$ complexes, which predominate in solution from acidic to slightly alkaline pH values, are totally unable to hydrolyze BNPP. These findings are in accord with the mechanism generally proposed for BNPP cleavage, which would involve a nucleophilic attack of a Zn–OH function. This mechanism also accounts for the lack of hydrolytic ability of the monohydroxo $[\text{Zn}_2\text{L}_2(\mu\text{-OH})]^{3+}$ complex, where the nucleophilic character of the hydroxide anion is strongly reduced by its bridging coordination to two electrophilic metal centers. Conversely, the two complexes $[\text{ZnL1}(\text{OH})]^+$ and $[\text{Zn}_2\text{L}_2(\text{OH})_2]^{2+}$ display a remarkable hydrolytic ability, far higher than that generally observed in BNPP cleavage promoted respectively by mono- and dinuclear Zn(II) complexes with polyamine ligands not containing aromatic subunits.^{41–49} This enhanced activity in BNPP cleavage can be attributed to the presence of the phenanthroline or dipyridine moieties, which can reinforce the overall interaction of the complexes with BNPP through hydrophobic interactions with the nitrophenyl groups of the substrate. Finally, the dinuclear $[\text{Zn}_2\text{L}_2(\text{OH})_2]^{2+}$ complex is remarkably more active than the mononuclear $[\text{ZnL1}(\text{OH})]^+$ one, in keeping with a cooperative role exerted by the two metals in the hydrolytic process, which takes place via a bridging interaction of BNPP.^{49b}

Both L1 and L2 complexes are also able to cleave supercoiled DNA affording its nicked circular form. Differently from BNPP, DNA cleavage occurs also at neutral pH, where the unique species present in solutions are the $[\text{ZnL1}]^{2+}$ complex and, in the case of L2, the $[\text{Zn}_2\text{L}_2\text{H}(\mu\text{-OH})]^{4+}$ and $[\text{Zn}_2\text{L}_2(\mu\text{-OH})]^{3+}$ complexes, which are virtually unable to cleave BNPP. At the same time, the L1 and L2 complexes display a similar hydrolytic efficiency, at least in low molar concentrations ($< 10 \mu\text{M}$), suggesting that the cooperative role of the two metals observed in BNPP hydrolysis promoted by the L2 complex is not present in DNA cleavage. These findings point out that DNA hydrolysis may take place through a different mechanism with respect to the simple “associative” process (interaction of the metal(s) with phosphate and simultaneous nucleophilic attack of a Zn(II)-bound hydroxide) proposed for BNPP. This prompted us to carry out a QM/MM study on the interaction of the L1 and L2 complexes with DNA. QM/MM calculations show that the $[\text{ZnL1}]^{2+}$ complex is placed within the minor groove of DNA, with the phenanthroline moiety close to the more hydrophobic zone of the nucleobases. Such a disposition enables the formation of a strong interaction between the Zn(II) ion and an oxygen atom of the phosphate group ($\text{Zn}\cdots\text{O} \ 2.14 \text{ \AA}$) and, at the same time, allows the Zn(II)-bound water molecule to stay at a rather close distance from phosphate ($\text{P}\cdots\text{OH}_2 \ 4.06 \text{ \AA}$). Therefore, both activation of the phosphate group, because of its interaction with zinc,

and presence of a metal-bound water molecule, a potential acid catalyst, at close distance from phosphate can favor the cleavage process.

Differently from $[\text{ZnL1}]^{2+}$, the $[\text{Zn}_2\text{L2H}(\mu\text{-OH})]^{4+}$ complex is located outside the minor groove. This different disposition can be related to the larger dimension of the L2 complex as well as to the lower hydrophobic characteristics of dipyridine than of phenanthroline and to the consequent lower tendency to insert in the minor groove. In this case, the complex/DNA interaction is featured by a very weak interaction of the anionic phosphate group with the two metals, only partially reinforced by a couple of hydrogen bonding interactions between two NH groups of the complex and two oxygen atoms of the same phosphate group. The bridging hydroxide anion has poor hydrolytic properties (see above) and at the same time, lies on the opposite side of the complex with respect to the phosphate group. Therefore, it seems unlikely that the Zn(II)-bound hydroxide can behave as a nucleophile in the hydrolytic process. Similarly, the Zn(II)-bound water and the NH_2^+ group are far from and not oriented toward phosphate, making improbable a general acid catalytic mechanism. These structural features suggest that the $[\text{Zn}_2\text{L2H}(\mu\text{-OH})]^{4+}$ complex would have scarce hydrolytic properties. Conversely, the $[\text{Zn}_2\text{L2}(\mu\text{-OH})]^{3+}$ /DNA adduct is featured by a strong interaction between a single Zn(II) ion of the complex and the phosphate group and by a short hydrogen bond contact between a phosphate oxygen and an amine group of the macrocycle ($\text{P}-\text{O}\cdots\text{H}-\text{N}$ 2.05 Å), which may lead to a higher activation of the phosphate group than in $[\text{Zn}_2\text{L2H}(\mu\text{-OH})]^{4+}$. The metal-bound hydroxide and water molecule still lie on the opposite side of the dimetal complex with respect to the phosphate group. Even if phosphate is more activated than in $[\text{Zn}_2\text{L2H}(\mu\text{-OH})]^{4+}$, the nucleophilic attack is likely to be due to an external water molecule or an hydroxide anion. In both complexes, however, the cooperative role of the two metals in substrate binding and activation, observed in BNPP hydrolysis, seems to be not working in DNA cleavage. This fact, together with the absence of either strongly nucleophilic Zn-OH or Zn-OH₂ molecules with the appropriate spatial disposition to act as acid catalysts, would account for a hydrolytic activity similar to that observed in the case of the mononuclear complex with L1, at least at neutral pH with low micromolar complex concentrations (<10 μM).

To corroborate this hypothesis, we coupled the QM/MM analysis on the adducts between DNA and the L1 and L2 hydroxo-complexes, formed in larger percentages in alkaline solutions, with cleavage experiments at different pH values (up to pH 9). In principle, an increasing amount in solutions of Zn-OH functions, more nucleophilic than Zn-bound water molecules, would lead to a higher activity in the hydrolysis of the phosphate ester bond, and actually, the hydrolysis rate of BNPP in the presence of both the L1 and L2 complexes increases with pH. The two complexes, instead, display a remarkably different pH-dependence of their hydrolytic ability toward DNA. In fact, while the activity of the L1 complex decreases with pH, the dinuclear Zn(II) complex shows an increasing efficiency in DNA cleavage as the pH

is raised from 6 to 9 (Figure 3), at least with low DNA concentrations. In the case of L1, the QM/MM study shows that both the *bent*- and *planar*- $[\text{ZnL1}(\text{OH})]^+$ complexes adopt a similar disposition with respect to DNA, with the phenanthroline moiety inserted within the minor groove. The *planar*- $[\text{ZnL1}(\text{OH})]^+$ complex, however, gives a remarkably more stable adduct with DNA than the *bent* conformer, suggesting that the *planar*- $[\text{ZnL1}(\text{OH})]^+$ /DNA adduct is the unique or at least prevalent species present in solution. This adduct is featured by a somewhat weaker interaction between phosphate and Zn(II) than in the $[\text{ZnL1}(\text{H}_2\text{O})]^{2+}$ /DNA adduct, and overall, the potential nucleophilic hydroxide group is located on the opposite side with respect to the phosphate group. Therefore, the formation of increasing percentages of the $[\text{ZnL1}(\text{OH})]^+$ species may account for the observed decreasing ability in DNA cleavage with increasing pH.

The dinuclear L2 complex displays a more common behavior, since its activity increases with pH, at least with low complex molar concentrations. In principle, this could be ascribed either to the formation of increasing amounts in alkaline solution of the $[\text{Zn}_2\text{L2}(\mu\text{-OH})]^{3+}$ complex, which gives a stronger interaction (and consequent higher activation) with a phosphate group than the $[\text{Zn}_2\text{L2H}(\mu\text{-OH})]^{4+}$ one, or to the formation of the $[\text{Zn}_2\text{L2}(\text{OH})_2]^{2+}$ complex, which contains a strongly nucleophilic Zn-OH function. On the other hand, QM/MM calculations show that in the DNA/ $[\text{Zn}_2\text{L2}(\text{OH})_2]^{2+}$ adduct the dimetal core is far from the phosphate group and therefore cannot induce phosphate activation. This suggests that the increased DNA cleavage observed at alkaline pH values is likely due to the DNA interaction with the $[\text{Zn}_2\text{L2}(\mu\text{-OH})]^{3+}$ complex, as well as to the presence of increasing amounts of hydroxide anions, which can act as external nucleophilic agents.

Concluding Remarks

The present study offers evidence for different mechanisms which can operate in BNPP and DNA cleavage promoted by Zn(II) complexes. In the case of BNPP, the hydrolytic ability of a complex is determined by substrate activation through interaction with the Zn(II) centers, as well as by the nucleophilic character of the Zn-OH functions. Actually, only the $[\text{ZnL1}(\text{OH})]^+$ and $[\text{Zn}_2\text{L2}(\text{OH})_2]^{2+}$ complexes, which contain strongly nucleophilic Zn-OH functions can hydrolyze BNPP. The species not containing or containing poorly nucleophilic Zn(II)-bound hydroxide anions ($[\text{ZnL1}(\text{H}_2\text{O})]^{2+}$, $[\text{Zn}_2\text{L2H}(\mu\text{-OH})]^{4+}$, and $[\text{Zn}_2\text{L2}(\mu\text{-OH})]^{3+}$) cannot cleave BNPP. Conversely, the latter complexes are able to hydrolyze DNA. In fact, the hydrolytic efficiency of these complexes toward DNA mainly depends on their ability to gain an optimal disposition within the DNA backbone, to achieve a strong activation of phosphate and a proper orientation of the Zn-OH₂ or Zn-OH functions. In this respect, subtle factors, such as dimension and hydrophobicity of the complex, contribute to determine the position and orientation of the complex with respect to the cleavable phosphate group. In the DNA adducts with the larger dinuclear complexes the Zn-OH or Zn-OH₂ groups are not properly disposed to be involved in the hydrolytic process

and therefore the nucleophilic attack is given by external water molecules or hydroxide anions. Conversely, the smaller and more hydrophobic mononuclear $[\text{ZnL1}(\text{H}_2\text{O})]^{2+}$ complex is placed within the DNA minor groove, achieving an appropriate position to strongly interact with a phosphate group and an optimal orientation of the Zn–OH₂ function to participate in the cleavage process. This structural characteristic may be a promising starting point to design Zn(II)-based specific cleavage agents which act through nonoxidative pathways at neutral pH. Actually, functionalization of the phenanthroline unit with site-specific targeting substructures (distamycin), also able to fit the DNA minor groove, can generate new bifunctional architectures combining effective scissoring ability with DNA sequence or structural specificity.

Experimental Section

Materials and Methods. Ligands L1 and L2 and their Zn(II) complexes were synthesized as previously reported.^{49b,53,55} DNA from calf thymus (ctDNA, highly polymerized sodium salt) was purchased from Sigma. Its concentration was determined using a molar extinction coefficient per residue of $6600 \text{ M}^{-1} \text{ cm}^{-1}$.⁵⁴ pBR 322 DNA (Fermentas) was used with no further purifications.

Kinetics of BNPP Hydrolysis. The hydrolysis rate of BNPP to give mono(*p*-nitrophenyl) phosphate (MNPP) and *p*-nitrophenate (the hydrolysis products were identified by means of ¹H and ³¹P NMR spectra) in the presence of the zinc complex with L1 was measured by an initial slope method monitoring the increase in 403 nm absorption of the *p*-nitrophenate at $308.1 \pm 0.1 \text{ K}$ using the procedure reported in ref 41. The ionic strength was adjusted to 0.1 with NMe_4NO_3 . MOPS (pH 6.5–8.5), TAPS (pH 7.8–9.1), and CHES (pH 8.6–10.1) buffers were used (50 mM). In a typical experiment, immediately after BNPP and the zinc complex with L1 were mixed in aqueous solutions at the appropriate pH (the reference experiment does not contain the Zn(II) complex), the UV absorption spectrum was recorded and followed generally until 5–10% decay of BNPP. A plot of the hydrolysis rate versus BNPP concentration (1–10 mM) at a given pH gave a straight line, and then we determine the slope/[zinc complex] as the second order rate constants k_{BNPP} ($\text{M}^{-1} \text{ s}^{-1}$). Plots of the k_{BNPP} values as a function of the molar concentration of the active species ($[\text{ZnL1}(\text{OH})]^+$) give a straight line and allow one to determine the k'_{BNPP} values for 100% formation of $[\text{ZnL1}(\text{OH})]^+$. Errors in k'_{BNPP} values were about 5%.

DNA Cleavage Experiments. DNA cleavage experiments were performed incubating pBR 322 (12 μM base pairs) at 37 °C in the presence/absence of increasing amounts of metal complex for 24 h in the required buffer (20 mM MES, pH 6.0; 20 mM HEPES, pH 7.0; 20 mM HEPES, pH 8.0; 20 mM TRIS, pH 9.0). Reaction products were resolved on a 1% agarose gel in TAE buffer (40 mM TRIS base, 20 mM, acetic acid, 1 mM EDTA) containing 1% SDS to dissociate the ligands from DNA. The resolved bands were visualized by ethidium bromide staining and photographed. The relative amounts of different plasmid structures were quantified using a BioRad Gel Doc 1000 apparatus interfaced to a PC workstation. The intensity of the band relative to the plasmid supercoiled form was multiplied by 1.43 to take into account its reduced affinity for ethidium bromide.

Unwinding Measurements. Supercoiled pBR322 DNA (0.15 μg) was incubated with 1 U of Topoisomerase I (Invitrogen) in 50 mM Tris·HCl, pH 7.5, 50 mM KCl, 10 mM MgCl₂, 0.5 mM DTT, 100 μM EDTA, 30 μg/ml BSA in the presence/absence of increasing concentrations of tested ligands. After o.n. incubation at 37 °C, NaCl was added to the samples to a final concentration of 0.15 M and, finally, extracted with an equal volume of 1:1 PhOH/CHCl₃ buffered to pH 7.5 with 50 mM Tris·HCl. The aqueous phases was loaded on 1% agarose gel, and run in TAE. The reaction products were visualized by ethidium bromide staining.

Light Scattering. Light scattering experiments were performed at 25 °C on a FL-20 Perkin-Elmer spectrofluorimeter equipped with a Haake F3–C thermostat using an excitation and emission wavelength of 360 nm. A 100 μM ctDNA solution was prepared in 20 mM HEPES, pH 7.0, and light intensity at 90° was measured after addition of increasing amounts of metal complex.

Circular Dichroism Measurements. The circular dichroism spectra of ctDNA were recorded from 230 to 320 nm in 20 mM HEPES, pH 7.0, using a 10 mm path length cell on a Jasco J 810 spectropolarimeter equipped with a NESLAB temperature controller. Incrementing concentrations of metal complex were added to a 100 μM DNA solution, and the mixtures were allowed to equilibrate 5 min before data acquisition. Every reported spectrum represents the average of 3 scans, recorded with 1-nm step resolution, for each sample. Observed ellipticities were converted to mean residue ellipticity $[\theta]$ expressed in $\text{deg} \times \text{cm}^2 \times \text{dmol}^{-1}$ (Molar Ell).

Molecular Modeling. Starting coordinates for $[\text{ZnL1}(\text{H}_2\text{O})]^{2+}$ and $[\text{Zn}_2\text{L2}]^{4+}$ were derived from a X-ray crystal structure analyses reported in previous works,^{49b,53} while starting coordinates for $[\text{Zn}_2\text{L2}(\text{OH})]^{3+}$ and $[\text{Zn}_2\text{L2}(\text{OH})_2]^{2+}$ were obtained by conformational search.⁵⁶ All conformations of the binuclear Zn/L2 complexes and that of $[\text{ZnL1}(\text{H}_2\text{O})]^{2+}$ were optimized by quantum-mechanical methods, DFT/B3LYP⁵⁷ level of theory with the LACVP* basis set,⁵⁸ which uses an effective core potential for the metal atom, while starting coordinates for the cis and trans conformations $[\text{ZnL1}(\text{OH})]^+$ were taken from a previous work^{49a} and not optimized. Fitting of the electrostatic potential (DFT/B3LYP level of theory with the LACVP* basis set) has been performed for all the docked compounds. The B-DNA structure for d-(5'-GCGCGCGCGC-3') polymer has been build up using the Builder module of Maestro.⁵⁹ The poses for the Zn(II)-complex/DNA adducts were obtained by rigid docking procedures carried out with GLIDE software.⁶⁰ Default input parameters were used in all computations (no scaling factor for the Van der Waals radii of non polar DNA atoms, 0.8 scaling factor for non polar ligand atoms). The grids for the docking (20 Å edges for the enclosing box) were centered on the centroid of the appropriate residues. Poses have been selected according to the highest electrostatic contribution to the overall energy. On equal, or similar, electrostatic terms, the poses featured by highest Van der Waals energetic term has been chosen.

(54) Fensenfeld, G.; Hirschmann, S. Z. *J. Mol. Biol.* **1965**, *13*, 407–427.
(55) Bencini, A.; Bianchi, A.; Fusi, V.; Giorgi, C.; Masotti, A.; Paoletti, P. *J. Org. Chem.* **2000**, *65*, 7686–7889.

(56) (a) Mohamadi, F.; Richards, N. G. J.; Guida, W. C.; Liskamp, R.; Lipton, M.; Caufield, C.; Chang, G.; Hendrickson, T.; Still, W. C. *J. Comput. Chem.* **1990**, *11*, 440–445. (b) *Macromodel*, v7.5; Schrödinger L.L.C: New York; <http://www.schrodinger.com>.
(57) (a) Becke, A. D. *J. Chem. Phys.* **1993**, *98*, 1372–1380. (b) Becke, A. D. *J. Chem. Phys.* **1993**, *98*, 5648–5657. (c) Lee, C.; Yang, W.; Parr, R. G. *Phys. Rev. B* **1988**, *37*, 785–780. (d) Miehlich, B.; Savin, A.; Stoll, H.; Preuss, H. *Chem. Phys. Lett.* **1989**, *157*, 200–208.
(58) Hay, P. J.; Wadt, W. R. *J. Chem. Phys.* **1985**, *82*, 299–308.
(59) *Maestro*, v7.5; Schrödinger L.L.C: New York; <http://www.schrodinger.com>.
(60) (a) Friesner, R. A.; Banks, J. L.; Murphy, R. B.; Halgren, T. A.; Klicic, J.; Mainz, D. T.; Repasky, M. P.; Knoll, E. H.; Shelley, M.; Perry, J. K.; Shaw, D. E.; Francis, P.; Shenkin, P. S. *J. Med. Chem.* **2004**, *47*, 1739–1749. (b) *Glide*, v3.5; Schrödinger L.L.C: New York; <http://www.schrodinger.com>.

Selected poses, representative of each interaction mode, were submitted to QM/MM optimizations performed by the Qsite software.⁶¹ This method adopts a quantum-mechanical (QM) treatment of the metal complexes, together with exogenous water molecules or hydroxo groups, which were treated at the DFT/B3LYP⁵⁵ level of theory with the LACVP* basis set,⁵⁸ while models the DNA duplex via a classical molecular mechanics force field (MM-OPLS2001 forcefield).⁶² Poisson–Boltzmann solver⁶³ has been applied to perform an implicit simulation of the aqueous solution.

(61) *Qsite*, v4.0; *Jaguar*, v6.5; Schrödinger L.L.C: New York, 2005; <http://www.schrodinger.com>.

(62) Jorgensen, W. L.; Maxwell, D. S.; Tirado-Rives, J. *J. Am. Chem. Soc.* **1996**, *118*, 11225–11235.

Supporting Information Available: Protonation constants of L1 and formation constants of the L1 complexes with Zn(II) at 308.1 K; experimental details for the potentiometric measurements on Zn(II) complexation with L1 at 308.1 K; lowest energy conformer of the $[\text{Zn}_2\text{L}2(\mu\text{-OH})(\text{OH})(\text{H}_2\text{O})]^{2+}$ complex (Figure S1) and lowest energy pose of the $[\text{Zn}_2\text{L}2(\mu\text{-OH})(\text{OH})]^{2+}$ /DNA adduct (Figure S2); atomic coordinates of the minimized Zn(II) complexes and their adducts with DNA (as xyz files). This material is available free of charge via the Internet at <http://pubs.acs.org>.

IC800085N

(63) Cortis, M. C.; Friesner, R. A. *J. Comput. Chem.* **1997**, *18*, 1591–1608.